Physica A 431 (2015) 74–83

Contents lists available at ScienceDirect

Physica A

journal homepage: www.elsevier.com/locate/physa

A semi-flexible attracting-segment model of three-dimensional polymer collapse

J. Krawczyk [a,b,*], A.L. Owczarek [c], T. Prellberg [d]

[a] Institute of Molecular Physics, Technical University of Łódź, 90-924 Łódź, Poland
[b] Department of Mathematical Sciences, Durham University, South Road, Durham DH1 3LE, United Kingdom
[c] Department of Mathematics and Statistics, The University of Melbourne, 3010, Australia
[d] School of Mathematical Sciences, Queen Mary University of London, Mile End Road, London E1 4NS, United Kingdom

HIGHLIGHTS

- Discussion on a three-dimensional semi-flexible AS model.
- Characterisation of one swollen and two collapsed phases.
- Characterisation of the transition between the phases.
- Discussion on the differences between two and three dimensional version of this model.

ARTICLE INFO

Article history:
Received 26 November 2014
Received in revised form 26 February 2015
Available online 10 March 2015

Keywords:
Polymer collapse
SAW
Attracting segments model
Stiff polymers
Semi-flexible polymers
Lattice polymers

ABSTRACT

Recently it has been shown that a two-dimensional model of self-attracting polymers based on attracting segments with the addition of stiffness displays three phases: a swollen phase, a globular, liquid-like phase, and an anisotropic crystal-like phase. Here, we consider the attracting segment model in three dimensions with the addition of stiffness. While we again identify a swollen and two distinct collapsed phases, we find that both collapsed phases are anisotropic, so that there is no phase in which the polymer resembles a disordered liquid drop. Moreover all the phase transitions are first order.

© 2015 Elsevier B.V. All rights reserved.

1. Introduction

An isolated polymer in solution undergoes a collapse transition from a swollen coil to a collapsed globule as the temperature is lowered and consequently the quality of the solvent is reduced. The canonical lattice model used to describe this scenario is the model of *Interacting Self-Avoiding Walks* (ISAW) on a regular lattice, such as the square or simple cubic lattice [1,2].

At high temperatures the self-avoiding walk is swollen, in that the fractal dimension of the walk d_f is less than the fractal dimension of simple random walks. The exponent $\nu = 1/d_f$ describes the scaling of the size of the walk, as measured for example by its radius of gyration, as a function of the length of the walk. It is known that $\nu = 3/4$ in two dimensions [3] and $\nu = 0.587597(7)$ in three dimensions [4].

* Corresponding author at: Institute of Molecular Physics, Technical University of Łódź, 90-924 Łódź, Poland.
E-mail address: jaroslaw.krawczyk@p.lodz.pl (J. Krawczyk).

http://dx.doi.org/10.1016/j.physa.2015.03.003
0378-4371/© 2015 Elsevier B.V. All rights reserved.

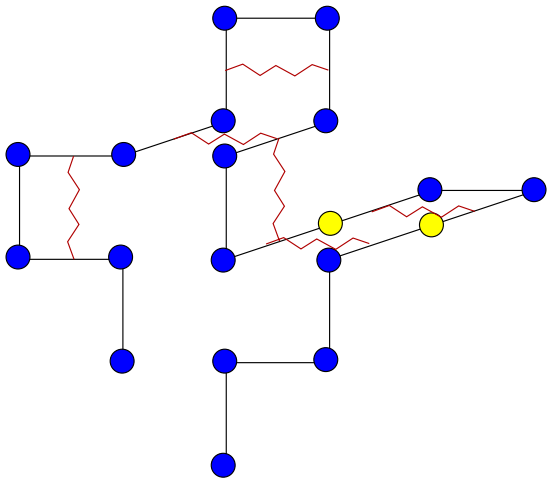

Fig. 1. A self-avoiding walk with the interactions of the attracting segment (AS) model shown as intertwined curves between bonds of the walk on opposite sides of the squares of the lattice. Also shown is an example of a stiffness segment pair which obtains a stiffness energy in our generalisation.

At low temperatures the self-avoiding walk is collapsed, in that the fractal dimension of the walk d_f is equal to the dimension d of the ambient space. The transition between the swollen coil and the collapsed globule happens at a particular temperature, called the θ-temperature.

In the standard description of the coil–globule transition, the transition is a tricritical point related to the $N \to 0$ limit of the φ^4–φ^6 O(N) field theory [5–7]; there is a second-order phase transition with a specific heat exponent conjectured to be $-1/3$ in two dimensions [8] and 0 in three dimensions with a logarithmic divergence of the specific heat. In two dimensions the fractal dimension of the walk is expected to be $d_f = 7/4$ [8] and $d_f = 2$ with logarithmic corrections in three dimensions.

The canonical model of interacting self-avoiding walks fits this scenario. In this model one expects the low-temperature state to be a liquid drop, i.e., the polymer is compact but disordered.

In stark contrast to this scenario, there is another simple interacting polymer model, the *Interacting Hydrogen-Bond* model (IHB) [9–11], where a pair of sites on the self-avoiding walk acquires a hydrogen-like bond potential if the sites are (non-consecutive) nearest neighbours, as in the ISAW model, and each site lies on a straight section of the walk. This model has been introduced in the context of biopolymers where hydrogen bonding plays an important role [12]. In contrast to ISAW, this model displays a first-order collapse transition in both two and three dimensions. Here, the low-temperature state is an anisotropic compact phase described as a polymer crystal.

Another model introduced to account for hydrogen bonding is the *Attracting Segments* model (AS) [13–15] (also known as 'interacting bonds'). It is a lattice model based on self-avoiding walks where an attractive potential is assigned to *bonds* of the walk that lie adjacent and parallel on the lattice (though not consecutive along the walk), see Fig. 1. On the square lattice, this model seems to have *two* phase transitions, one of which is identified as the θ-point [15].

If one introduces stiffness into the ISAW model, one arrives at the *semi-flexible* ISAW model [16–19]. In addition to the nearest-neighbour site interaction of ISAW, one introduces a stiffness energy associated with consecutive parallel bonds of the walk. This was studied on the cubic lattice by Bastolla and Grassberger [16], where it was shown that depending on the energetic weighting of straight segments one finds a single first-order transition from a swollen coil to a crystalline state for a strong energetic preference for straight segments, or a soft θ-transition from a swollen coil to a liquid globule, followed by a first-order transition to a crystalline state. In two dimensions, a similar scenario has been found [20], the main difference being that the transition between the globule and the frozen state becomes second-order.

The semi-flexible AS model, in which both straight segments and interacting segments carry an energy, as shown in Fig. 1, has been studied in two dimensions in Ref. [21], where it was found that it has a phase structure in common with the semi-flexible ISAW model.

In this paper, we discuss the semi-flexible AS model in three dimensions. While we again identify a swollen and two distinct collapsed phases, we find that both collapsed phases are anisotropic, so that there is no phase in which the polymer resembles a disordered liquid drop. The transitions between the swollen and each of the collapsed phases and between the two collapsed phases are first order. The three lines of transitions in parameter space meet at a triple point.

2. Our study

2.1. Semi-flexible attracting segments model

Our semi-flexible attracting segments model (semi-flexible AS model) is a self-avoiding walk on the simple cubic lattice, with self-interactions as in the AS model [13–15] and a stiffness (or equivalently bend energy) added. Specifically, the energy

of a single chain (walk) consists of two contributions (see Fig. 1): the energy $-\varepsilon_{as}$ for each attracting segment pair, being a pair of occupied bonds of the lattice that are adjacent and parallel on the lattice and not consecutive along the walk; and an energy $-\varepsilon_{ss}$ for each stiffness segment pair, being a pair of bonds consecutive along the walk that are parallel. A walk configuration φ_n of length n has total energy

$$E_n(\varphi_n) = -m_{as}(\varphi_n)\,\varepsilon_{as} - m_{ss}(\varphi_n)\,\varepsilon_{ss}, \tag{2.1}$$

where m_{as} denotes the number of attracting segment pairs and m_{ss} denotes the number of stiffness segment pairs. The partition function is defined then as

$$Z_n(\beta_{as}, \beta_{ss}) = \sum_{m_{as},m_{ss}} C_{n,m_{as},m_{ss}} \mathrm{e}^{\beta_{as}m_{as}+\beta_{ss}m_{ss}}, \tag{2.2}$$

where $\beta_{as} = \varepsilon_{as}/k_BT$ and $\beta_{ss} = \varepsilon_{ss}/k_BT$ for temperature T and Boltzmann constant k_B. The density of states, $C_{n,m_{as},m_{ss}}$, has been estimated by means of Monte Carlo simulations.

2.2. Simulations

On the cubic lattice we performed simulations using the FlatPERM algorithm [22], estimating the density of states up lengths for $n = 128$ over the two parameters m_{as} and m_{ss}. We use averages for the density of states from five independent runs. Moreover, we have simulated the density of states in m_{as} at $\beta_{ss} = \pm 1.0$ and in m_{ss} at $\beta_{as} = 1.0$ for lengths up to $n = 256$.

The density of states allows us to calculate the internal energy and the specific heat, or equivalently, the mean values and the fluctuations of m_{as} and m_{ss}, respectively. This allows us to locate phase transitions through the possible divergences in the specific heat. To detect orientational order, we estimated an *anisotropy parameter* [16].

3. Results

3.1. Phase diagram

From the density of states for 128-step walks, we compute the expected number of attracting segment pairs and stiff segment pairs, shown in Fig. 2 as a function of β_{as} and β_{ss}. There are three distinct regions recognisable. For small values of β_{as} both $\langle m_{as}\rangle$ and $\langle m_{ss}\rangle$ are small, with $\langle m_{ss}\rangle$ increasing slowly as β_{ss} increases. Upon increasing β_{as}, there is a sharp transition to large values of $\langle m_{as}\rangle$, indicative that the walks are collapsed on average. For large β_{as} the density of straight segments, $\langle m_{ss}\rangle$, is small for negative values of β_{ss}, but increases sharply as β_{ss} increases. This indicates that there are two distinct phases when β_{as} is large (collapsed region).

Putting this broad information together it seems to indicate that there is a region in which the walk forms a swollen coil (the non-interacting SAW at $\beta_{as} = \beta_{ss} = 0.0$ lies in this region), and that there are two regions in which the walk is collapsed. For one of the collapsed regions with negative β_{ss}, $\langle m_{as}\rangle$ is very small (in fact smaller than in the swollen region for the same values of β_{as}), whereas for the other collapsed region with positive β_{ss}, $\langle m_{as}\rangle$ is large.

The fluctuations $\sigma^2(m_{as})$ and $\sigma^2(m_{ss})$, also shown in Fig. 2, confirm this scenario. The fluctuations of m_{as} sharply peak upon increasing β_{as}. This peak is stronger for positive values of β_{ss}, where it is matched by a peak in the fluctuations of m_{ss}. For negative values, it is weaker, and there is no matching peak in the fluctuations of m_{ss}. This indicates that there are two different transitions from the swollen region to the collapsed region. Moreover, within the collapsed region we find a sharp peak in the fluctuations in m_{ss} upon increasing β_{ss}, which is not matched by a peak in the fluctuations of m_{as}.

We thus have three clearly defined regions in the β_{as}, β_{ss}-plane, delineated by rather sharp peaks in fluctuations. The presence of these fluctuations leads us to identify these regions with thermodynamic phases, so that we have a swollen globular phase, and two collapsed phases, one of which is rich in straight segments, and one of which is rich in bends. The conjectured phase diagram is shown in Fig. 3. This phase diagram also indicates that the transition lines are first-order, and that the collapsed phases have in fact a crystalline structure. We will provide evidence for this in the next two sections.

3.2. Phase transitions

In order to study the order of the three transitions, we consider the behaviour of the system on the straight lines $\beta_{ss} = 1.0$, $\beta_{ss} = -1.0$, and $\beta_{as} = 1.8$, which have been chosen to cut across the three different phase transition lines. In Fig. 4 we show the scaled fluctuations $\sigma^2(m_{as})/n^2$ and $\sigma^2(m_{ss})/n^2$, which behave according to the finite-size scaling of the first order transition [23,24]. The scaling has been chosen such that the peak height should tend to a constant if the transition is first-order. Clearly all three lines show strong transitions, and to clarify whether they are really first-order we consider the distribution of the appropriate microcanonical parameters.

In Fig. 5 we show the distribution of m_{as} at the peak of its fluctuation in β_{as} along the lines $\beta_{ss} = 1.0$ and $\beta_{ss} = -1.0$, and the distribution of m_{ss} at the peak of its fluctuation in β_{ss} along the line $\beta_{as} = 1.8$. The distribution along $\beta_{ss} = 1.0$ is clearly bimodal with the distance between the double peaks slightly widening as n changes from 128 to 256. This confirms the first-order nature of that transition, and also explains why the fluctuation peak grows super-linearly in Fig. 4. Along the line

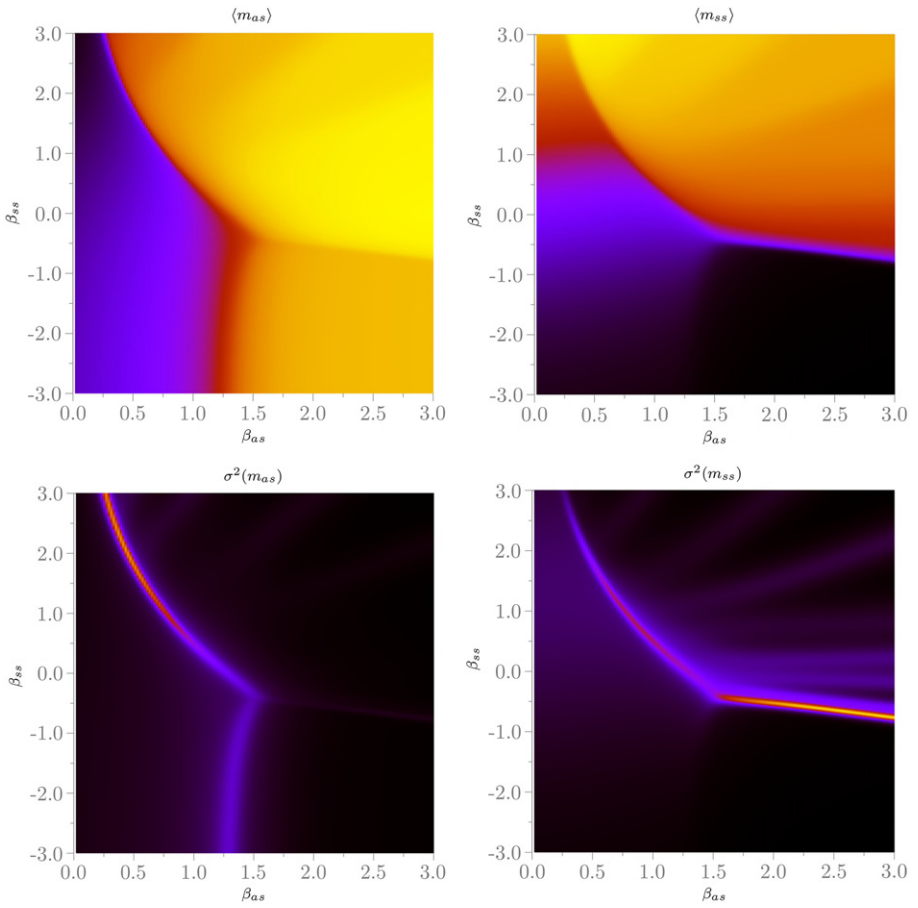

Fig. 2. Expected value of the number of attracting segments pairs m_{as} (top left) and stiff segment pairs m_{ss} (top right) and their fluctuations $\sigma^2(m_{as})$ (bottom left) and $\sigma^2(m_{ss})$ (bottom right) for 128-step walks as a function of β_{as} and β_{ss}.

$\beta_{ss} = -1.0$ we also find an emerging double peak, albeit developing at much longer lengths. Finally, along the line $\beta_{as} = 1.8$ we find a bimodal distribution with one peak located very closely to $m_{ss} = 0$. (Since we have not performed simulations for bigger systems for the line $\beta_{as} = 1.8$ we use the data from the simulations for n up to 128.) Hence, we conclude that the transitions between all three phases are first-order.

3.3. Nature of the collapsed phases

We now turn to the investigation of the two collapsed phases. As in Ref. [21], it will be helpful to consider an anisotropy parameter. In three dimensions, denoting the number of bonds parallel to the x-, y-, and z-axes by n_x, n_y, and n_z, respectively, we define

$$\rho = 1.0 - \frac{\min(n_x, n_y, n_z)}{\max(n_x, n_y, n_z)} \tag{3.1}$$

to be the anisotropy parameter. In a system without orientational order, this quantity tends to zero as the system size increases. A non-zero limiting value less than one of this quantity indicates weak orientational order with $n_{\min} \propto n_{\max}$, while a limiting value of one indicates strong orientational order, where $n_{\max} \gg n_{\min}$.

We first consider the change of the anisotropy parameter as the phase boundaries are crossed along the same three lines investigated earlier. This is shown in Fig. 6 for $\beta_{ss} = 1.0$, in Fig. 7 for $\beta_{ss} = -1.0$, and in Fig. 8 for $\beta_{as} = 1.8$, together with the corresponding changes of the density of interacting segments $\langle m_{as}\rangle$ and straight segments $\langle m_{ss}\rangle$.

In addition to the change in $\langle m_{as}\rangle$ and $\langle m_{ss}\rangle$ described above, one sees that the anisotropy parameter decreases in the swollen phase, but jumps to a significantly larger value in the collapsed phases. There is a small difference in the value of the anisotropy parameter in both collapsed phases, but the change of ρ as the length of the walk increases is such that ρ might in fact tend to the same limiting value of one in the thermodynamic limit.

To test this, we now display the finite-size scaling behaviour at two points in the different collapsed phases. The values $\langle m_{ss}\rangle/n$, $\langle m_{as}\rangle/n$ and ρ are shown as functions of $n^{-2/3}$ for $\beta_{as} = 1.4$ and $\beta_{ss} = 1.0$ in Fig. 9 and for $\beta_{as} = 1.8$ and $\beta_{ss} = -1.0$

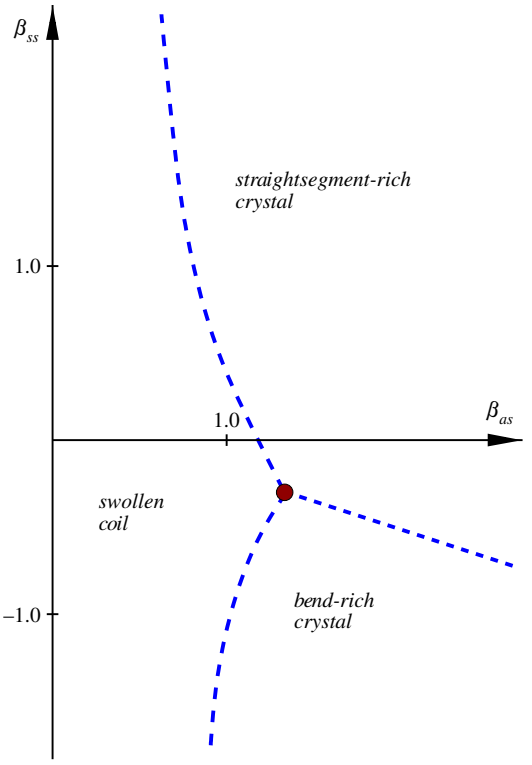

Fig. 3. A sketch of the conjectured phase diagram, showing the swollen globular phase and the two crystalline phases. The three phase transition lines (dashed blue) are all first-order and meet in a common critical point (red).

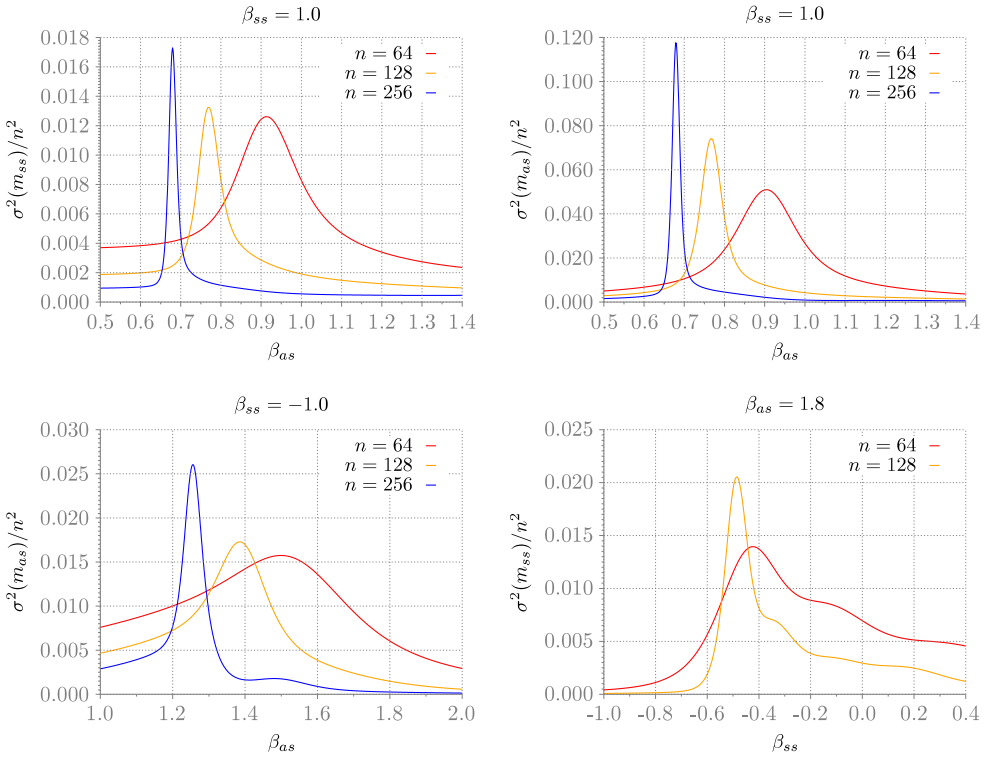

Fig. 4. Scaled fluctuations in m_{ss} and m_{as} on the line $\beta_{ss} = 1.0$ (top left and right, respectively), scaled fluctuations in m_{as} on the line $\beta_{ss} = 1.0$ (bottom left) and scaled fluctuations in m_{ss} on the line $\beta_{as} = 1.8$ (bottom right).

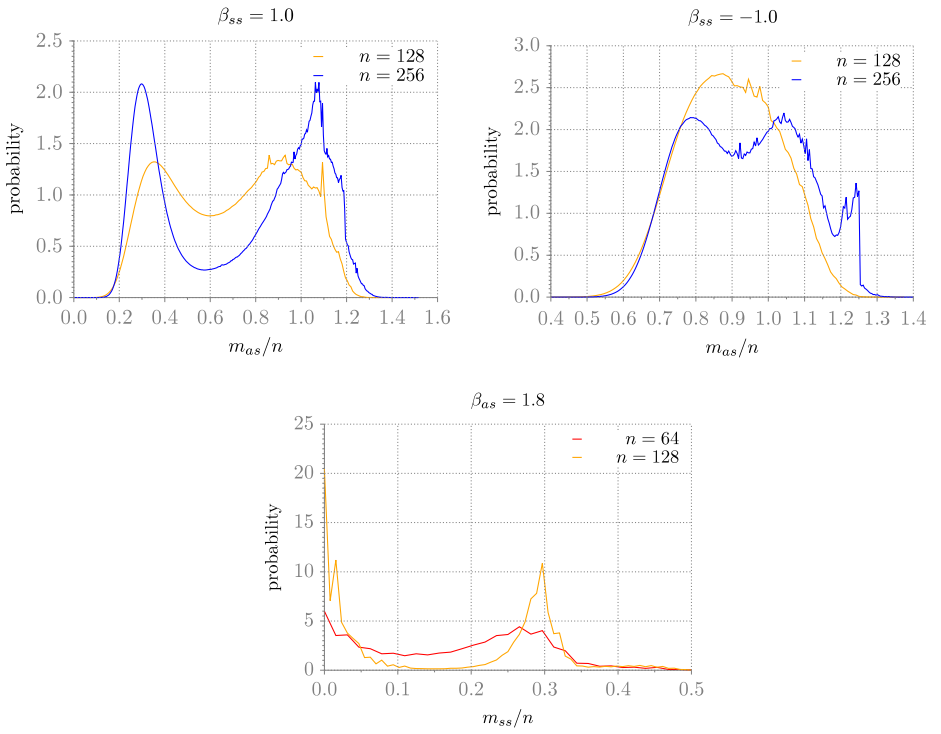

Fig. 5. The top two figures show the scaled distributions of m_{as} for $\beta_{ss} = 1.0$ and $\beta_{ss} = -1.0$ (top left and right, respectively), for walk lengths $n = 128$ and $n = 256$, with the values of β_{as} chosen such that the fluctuations in m_{as} were maximal (for $\beta_{ss} = 1.0$, $\beta_{as} = 0.770$ and 0.681 for $n = 128$ and 256, respectively), and for $\beta_{ss} = -1.0$, $\beta_{as} = 1.382$ and 1.254 for $n = 128$ and $n = 256$, respectively. The bottom figure shows the scaled distributions of m_{ss} for $\beta_{as} = -1.8$ for walk lengths $n = 64$ and $n = 128$, with the values of β_{ss} chosen such that the fluctuations in m_{ss} were maximal ($\beta_{ss} = -0.420$ and -0.487 for $n = 64$ and $n = 128$, respectively).

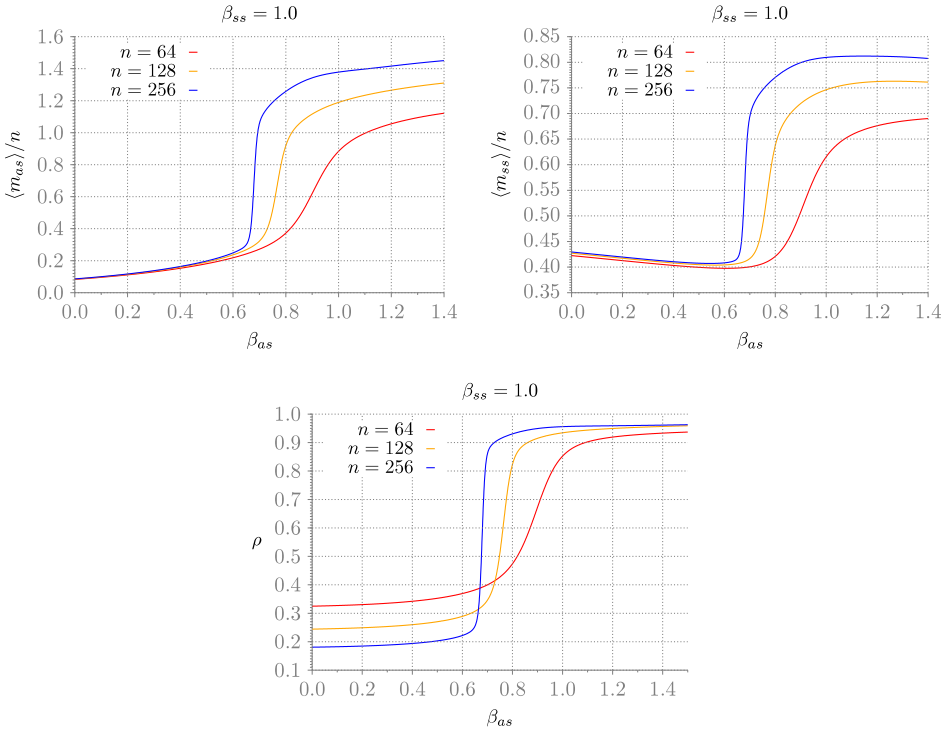

Fig. 6. Line $\beta_{ss} = 1.0$. The scaled number of contacts $\langle m_{as}\rangle$ and $\langle m_{ss}\rangle$ and anisotropy parameter as a function of β_{as} for constant $\beta_{ss} = 1.0$ for three system sizes $n = 64$, 128 and 256.

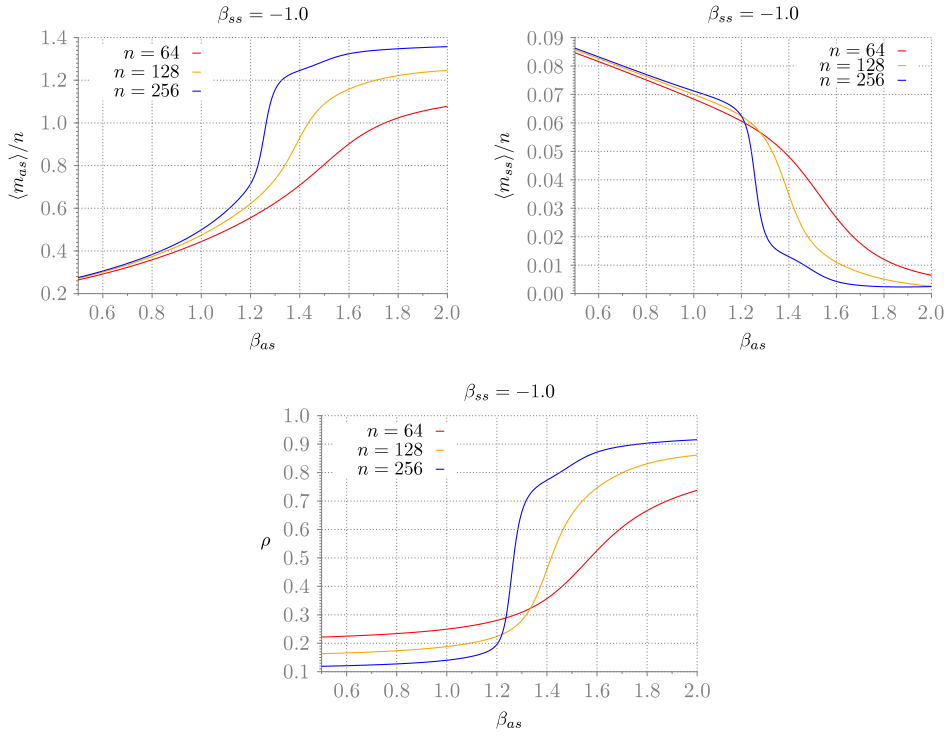

Fig. 7. Line $\beta_{ss} = -1.0$. The scaled number of contacts $\langle m_{as}\rangle$ and $\langle m_{ss}\rangle$ and anisotropy parameter as a function of β_{as} for constant $\beta_{ss} = -1.0$ for three system sizes $n = 64$, 128 and 256.

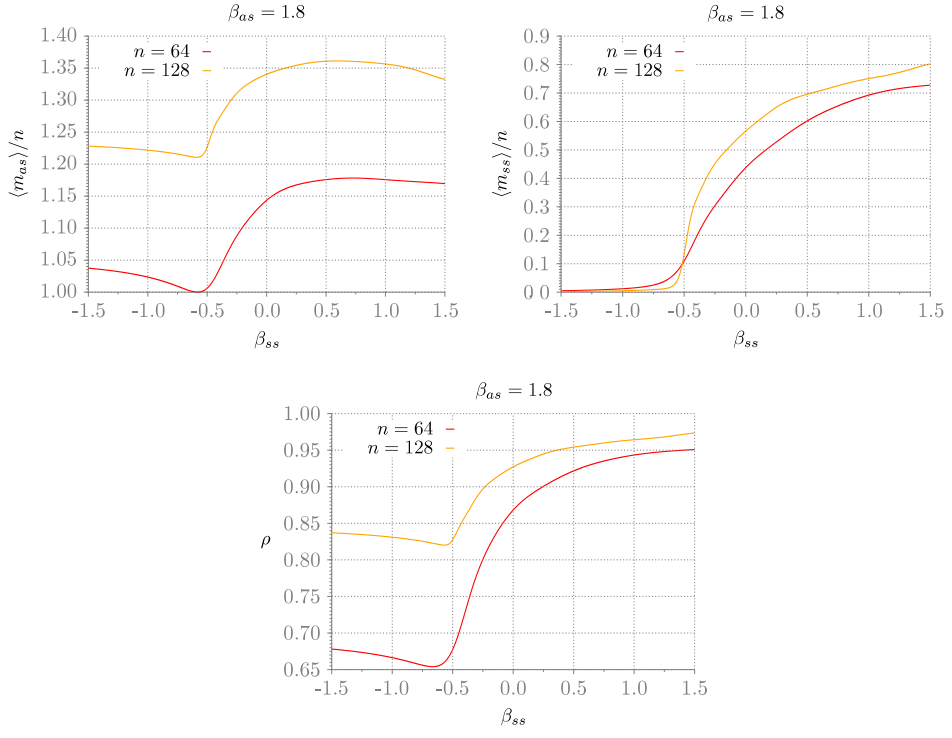

Fig. 8. Line $\beta_{as} = 1.8$. The scaled number of contacts $\langle m_{as}\rangle$ and $\langle m_{ss}\rangle$ and anisotropy parameter as a function of β_{ss} for constant $\beta_{as} = 1.8$ for two system sizes $n = 64$ and 128. The decrease of the anisotropy parameter close to $\beta_{ss} = -0.6$ is due the fluctuations at the phase transition.

in Fig. 10. If the corrections to scaling are due to surface effects, one should find asymptotic straight lines as $n^{-2/3}$ tends to zero.

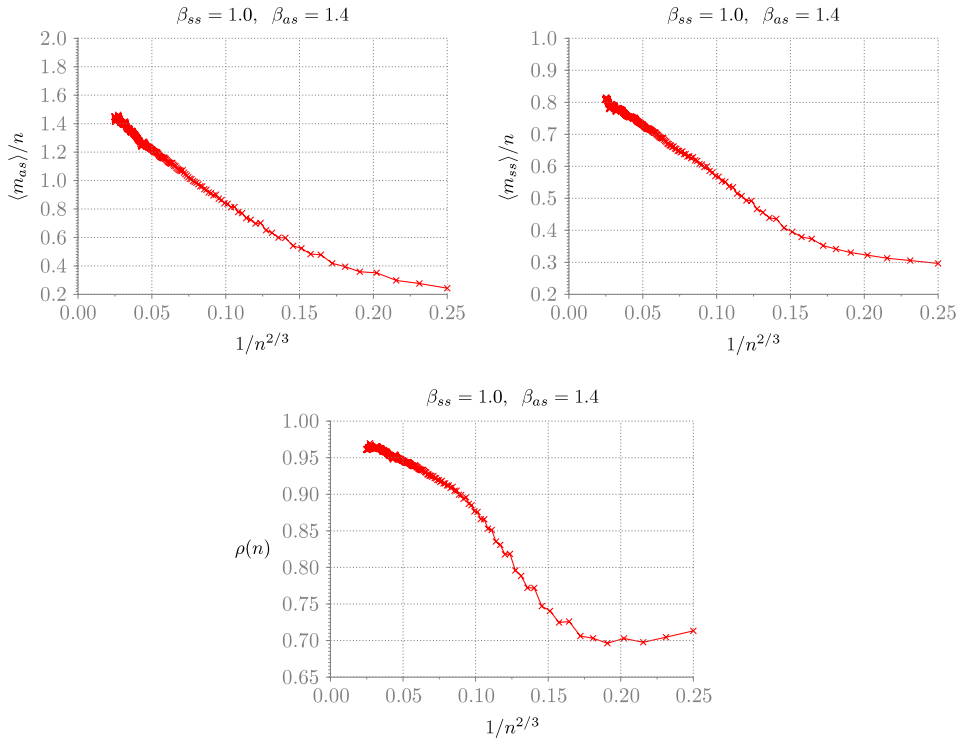

Fig. 9. Number of contacts $\langle m_{ss} \rangle / n$ and $\langle m_{as} \rangle / n$ and anisotropy parameter, ρ, as function of the system size at $\beta_{as} = 1.4$ and $\beta_{ss} = 1.0$. Importantly, the anisotropy parameter, ρ, can be seen to converge to $\rho = 1$ for infinite n within error. The thermodynamic average of straight segments converges to a value near 0.9 within error.

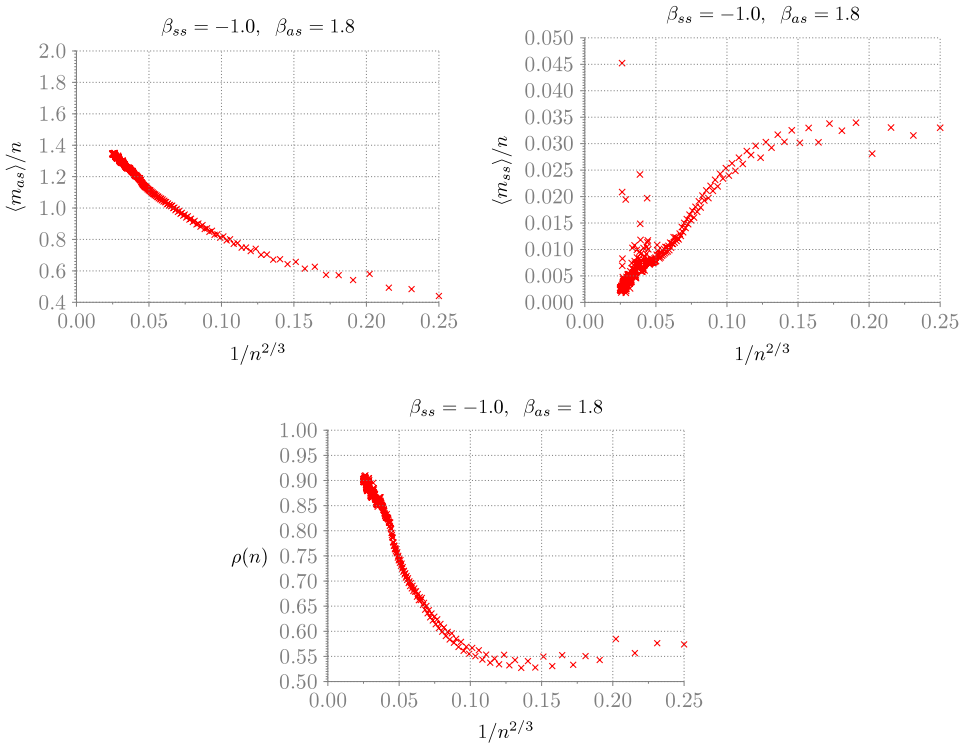

Fig. 10. Number of contacts $\langle m_{ss} \rangle / n$ and $\langle m_{as} \rangle / n$ and anisotropy parameter, ρ, as function of the system size at $\beta_{as} = 1.8$ and $\beta_{ss} = -1.0$. Importantly, the anisotropy parameter, ρ, can be seen to converge to $\rho = 1$ for infinite n within error and the thermodynamic average of straight segments converges to $\lim_{n\to\infty} \langle m_{ss} \rangle / n = 0$ within error.

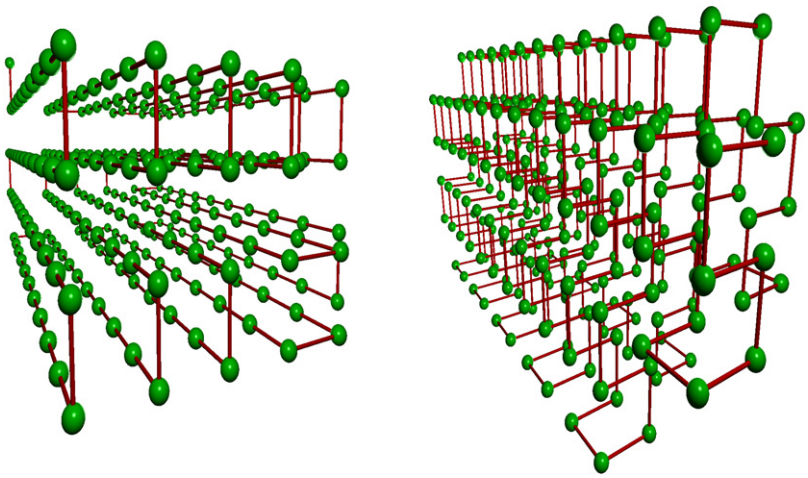

Fig. 11. Typical configurations of length 128 at the parameter values $(\beta_{as}, \beta_{ss}) = (1.4, 1.0)$ (left) and $(\beta_{as}, \beta_{ss}) = (1.8, -1.0)$ (right). The configuration on the left is an array of long straight lines of monomers while the configuration on the right contains mainly bends.

Both figures confirm the presence of $n^{-2/3}$-corrections, indicating a well-developed surface of the collapsed walk. The anisotropy parameter tends to one in both phases in the thermodynamic limit, indicating crystalline order. However, in one phase the density of straight segments tends to a limiting value close to one, whereas in the other phase this quantity tends to zero, showing clear evidence of two structurally very different crystalline structures, each of which has a different limiting density of attracting segments.

This scenario is confirmed by Fig. 11, which shows typical configurations at these two parameter values: in the straight-rich phase, $(\beta_{as}, \beta_{ss}) = (1.4, 1.0)$, the typical configurations consist of straight lines of monomers while in the bend rich phase, $(\beta_{as}, \beta_{ss}) = (1.8, -1.0)$, the typical configuration can be described as parallel sheets of two-dimensional configurations consisting only of bends. The limiting value of $\langle m_{as}\rangle/n$ is equal to 2 in the former phase, and equal to $7/4$ in the latter phase, consistent with the numerical data shown in Figs. 9 and 10.

The bend-rich-crystal phase consists of two-dimensional sheets of bended chains which lie parallel to each other. While the two dimensional sheets are isotropic. The ordering of those sheets induces the anisotropy of the phase. In general, the difference in the behaviour of this model between dimensions lies to some extent in the freedom that three dimensions afford the lattice polymer to form different crystalline structures. Transitions to such rigid structures tend to be first order.

In this article we have discussed a three-dimensional semi-flexible AS model. We have characterised one swollen and two collapsed phases, and transition between them. In contrast to the two dimensional version of this model, both collapsed phases are anisotropic, and none of them resemble the disordered liquid drop.

Acknowledgements

Financial support from the Australian Research Council (Grant number DP120101593) via its support for the Centre of Excellence for Mathematics and Statistics of Complex Systems and via its Discovery program is gratefully acknowledged by the authors. A.L. Owczarek thanks the School of Mathematical Sciences, Queen Mary University of London for hospitality. This research was supported in part by Polish Grid Infrastructure.

References

[1] W.J.C. Orr, Trans. Faraday Soc. 43 (1947) 12.
[2] C. Vanderzande, A.L. Stella, F. Seno, Phys. Rev. Lett. 67 (1991) 2757.
[3] B. Nienhuis, Phys. Rev. Lett. 49 (1982) 1062.
[4] N. Clisby, Phys. Rev. Lett. 104 (2010) 055702.
[5] P.-G. de Gennes, J. Physique Lett. 36 (1975) L55.
[6] M.J. Stephen, Phys. Lett. A 53 (1975) 363.
[7] B. Duplantier, J. Physique 43 (1982) 991.
[8] B. Duplantier, H. Saleur, Phys. Rev. Lett. 59 (1987) 539.
[9] J. Bascle, T. Garel, H. Orland, J. Phys. II France 3 (1993) 245.
[10] D.P. Foster, F. Seno, J. Phys. A 34 (2001) 9939.
[11] J. Krawczyk, A.L. Owczarek, T. Prellberg, A. Rechnitzer, Phys. Rev. E (2007) 051904:1.
[12] L. Pauling, R.B. Corey, Proc. Natl. Acad. Sci. 37 (1951) 235, 251, 272.
[13] K.D. Machado, M.J. Oliveira, J.F. Stilck, Phys. Rev. E 64 (2001) 051810.
[14] C. Buzano, M. Pretti, J. Chem. Phys. 117 (2002) 10360.
[15] D.P. Foster, J. Phys. A: Math. Theor. 40 (2007) 1963.
[16] U. Bastolla, P. Grassberger, J. Stat. Phys. 89 (1997) 1061.
[17] A.M.S. Lise, A. Pelizzola, Phys. Rev. E 58 (1998) R5241.

[18] T. Vogel, M. Bachmann, W. Janke, Phys. Rev. E 76 (2007) 061803.
[19] J.P.K. Doye, R.P. Sear, D. Frenkel, J. Chem. Phys. 108 (1997) 2134.
[20] J. Krawczyk, A.L. Owczarek, T. Prellberg, Physica A 388 (2008) 104.
[21] J. Krawczyk, A.L. Owczarek, T. Prellberg, Physica A 389 (2009) 1619.
[22] T. Prellberg, J. Krawczyk, Phys. Rev. Lett. 92 (2004) 120602.
[23] M.E. Fisher, A.N. Baker, Phys. Rev. B 26 (1982) 2507.
[24] V. Privman, M.E. Fisher, J. Stat. Phys. 33 (1983) 385.